Feasibility and effects of a self-assembling peptide as a scaffold in bone healing: An in vivo study in rabbit lumbar posterolateral fusion and tibial intramedullary models

Kei Ando, MD, PhD [a], Shiro Imagama, MD,PhD [a] *, Kazuyoshi Kobayashi, MD,PhD [a], Kenyu Ito, MD, PhD [a] , Mikito Tsushima, MD, PhD [a] , Masayoshi Morozumi, MD, PhD [a] , Satoshi Tanaka, MD, PhD [a] , Masaaki Machino, MD, PhD [a] , Kyotaro Ota, MD, PhD [a] , Koji Nishida, MD,PhD [b], Yoshihiro Nishida, MD,PhD [a], Naoki Ishiguro, MD,PhD [a]

[a] Department of Orthopedic Surgery, Nagoya University Graduate School of Medicine, 65 Tsurumai-cho, Showa-ku, Nagoya, Aichi 466-8550, Japan
Phone: +81-52-741-2111
Fax: +81-52-744-2260

[b] Department of Ophthalmology, Osaka University Graduate School of Medicine, Suita, Osaka, Japan

Author contributions: Study design: SI, KN, YN, and NI, Data collection: KK and KI, Data interpretation: MT, MM, ST, and MM, Drafting manuscript: KO. All authors have read and approved the final submitted manuscript.

* Correspondence: Shiro Imagama, Department of Orthopedic Surgery, Nagoya University Graduate School of Medicine, 65 Tsurumai-cho, Showa-ku, Nagoya, Aichi 466-8550, Japan
Phone: +81-52-741-2111, E-mail: imagama@med.nagoya-u.ac.jp

Graphical abstract

Spinal fusion and bone defects after injuries, removal of bone tumors, and infections require repair by implantation. We show SPG-178 hydrogel-induced bone healing *in vivo*. In the tibia model, SEM/3D micrographs showed that the cavity filled with self-assembling peptide (SPG-178) hydrogel had collagen fibers attached to host bone. After 28 days, samples from the SPG-178 group showed significant repair of the defect. These include its favorable bone conduction properties, its ability to act as a support for various cells.

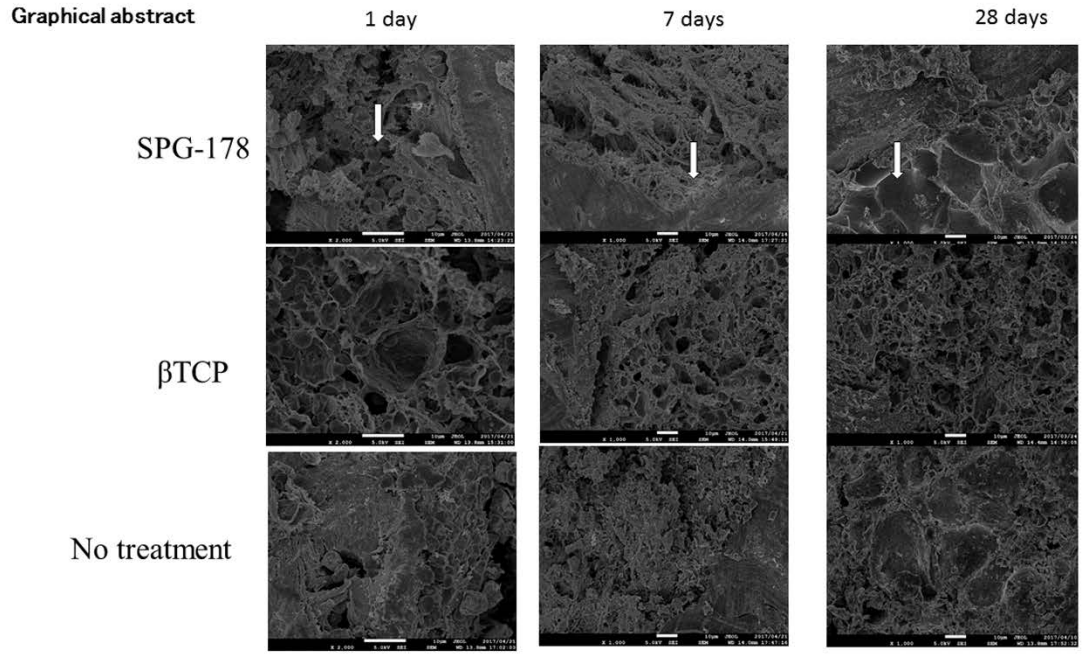

Abstract

Spinal fusion and bone defects after injuries, removal of bone tumors, and infections require repair by implantation. In this study, we show self-assembling peptide (SPG-178) hydrogel-induced bone healing *in vivo*. Posterolateral lumbar fusion and tibial intramedullary models of rabbits were prepared. In the tibia model, micro-CT analysis revealed a significantly higher degree of newly formed bone matrix in the SPG-178 group compared to the other groups. SEM/3D micrographs showed that the cavity filled with SPG-178 had collagen fibers attached to host bone. After 28 days, samples from the SPG-178 group showed significant repair of the defect. In the posterolateral lumbar fusion models, micro-CT showed a tendency for a higher degree of newly formed bone matrix in the SPG-178 group compared to the β-TCP and bone chips only groups. Von Kossa staining showed marked new bone formation attached to the lamina that was most prominent at the implanted SPG-178 composite margin. SPG-178 is a material that is likely to be used in clinical applications because it has several benefits. These include its favorable bone conduction properties, its ability to act as a support for various cells and growth factors, its lack of infection risk compared with materials of animal origin such as ECM, and the ease with which it can be used to fill defects with complex shapes and be combined with a wide range of other materials.

Key words

self-assembling peptide

scaffold

bone healing

Introduction

Spinal compression fractures and femoral neck fractures due to osteoporosis have increased with aging of society. Surgical outcomes have improved as a result of advances in implants[7,13], but bony union is necessary to prevent implant failure due to pseudoarthrosis[9]. For promotion of union, a bone substitute is often used to provide a scaffold for regeneration of the new bone. Autografts with augmentation using metal devices are performed because of their superior osteoinductivity and osteoconductivity. However, autograft bone is often limited in supply and may also be associated with donor site morbidity[6]. Therefore, tissue engineering products have emerged as an alternative approach to regeneration of bone[20,24]. Hydroxyapatite (HA) and tricalcium phosphate (TCP) as synthetic calcium phosphates are commonly used as bone substitutes[4,15]. These materials have excellent biocompatibility and osteoinductivity with the bony environment[12,27], but a gap may develop between the grafted bone and bone substitute because of the solid nature of the material, which may result in pseudoarthrosis[25].

Self-assembling peptides are candidate materials to solve these problems. The complete sequence of a self-assembling peptide was originally found in a region of alternating hydrophobic and hydrophilic residues in zuotin[31], which is has a stable β-sheet structure that undergoes self-assembly into nanofibers. These nanofibers form interwoven matrices that then form a hydrogel scaffold[29,32]. These hydrogel systems are well characterized and have been used in tissue engineering studies[5,8,10,22] and as drug delivery systems[17]. The self-assembling peptides are also fully synthetic material, which minimizes the risk of biological contamination and the influence of undefined factors in use of the hydrogels. Moreover, a particularly attractive feature of a hydrogel is that it can penetrate through bone, whereas this is not possible for a solid substitute.

We have developed an artificial self-assembling peptide, SPG-178 (Self-assembling Peptide Gel, amino acid sequence #178; [CH_3CONH]-RLDLRLALRLDLR-[$CONH_2$]; R = arginine, L = leucine, D = aspartic acid, A = alanine) as a scaffold and potential therapeutic agent for treatment of spinal cord injury (SCI)[1]. Peptides are administered as hydrogels, which is advantageous compared to materials such as β-TCP and HA that are used as solids, in that the peptide hydrogel is injectable, can fill space between grafted bones, and has excellent biocompatibility[30]. The generated nanofibers mimic the natural extracellular matrix (ECM) and enhance attachment, growth and differentiation of a variety of cells, including chondrocytes and osteoblasts[2,14]. The

stability of the peptide solution/hydrogel at neutral pH contributes to the biocompatibility of the scaffold and provides an additional benefit in the sterilization procedure [18]. In this study, we show improved bone healing with use of SPG-178 in rabbit posterolateral lumbar fusion and tibial intramedullary models. The results provide new evidence for the role of SPG-178 as a scaffold for osteogenesis through induction of osteoconductive factors.

Materials and Methods

Materials

The self-assembling peptide SPG-178, [CH3CONH]-RLDLRLALRLDLR-[CONH2], was purchased from Menicon Corp., Nagoya, Japan. It was synthesized by a solid-phase method using a standard Fmoc strategy[18]. The peptide powder was dissolved in a 10% (w/v) sucrose solution. The peptide solution was sterilized by filtration through a 0.22-mm filter and then adjusted to approximately pH 6.5 by adding aliquots of 0.5% (w/v) sodium hydrogen carbonate solution. The final concentration of the peptide in the solution was 2.4 mM (0.4% w/v).

Animals

Kbl:JW rabbits of age 20 weeks and weight 3-3.5 kg (Kitayama Kabes Co., Nagano, Japan) were used in all procedures. Animal experiments were performed in strict accordance with the Guide for the Care and Use of Laboratory Animals (National Research Council, 1996) and all efforts were made to minimize suffering. All animal procedures were approved by the Institutional Animal Care and Use Committee of Nagoya University for the use of laboratory animals. For allogeneic bone, femurs of other rabbits were smashed into pieces to produce bone chips.

Preparation of allogenic bone chips

Two femurs taken from a donor animal sacrificed with a lethal anesthetic dose were used to prepare bone chips. The bones were immediately separated from soft tissues, including cartilage and periosteum. After removal of the distal epiphysis, the bones were smashed into pieces to produce bone chips, which were then frozen and stored at -80°. Two weeks before surgery the bone chips were sterilized with ethylene oxide gas and stored at room temperature for aeration to remove residual oxide and its breakdown products.

Tibial intramedullary model

Under sterile conditions, an anteromedial incision was made in the proximal rabbit tibia. The muscles were divided and the medial condyle of the tibia was exposed. Cylindrical bone defects of non-critical size (5-mm diameter and 5-mm depth) were made in the medial face of the tibia using a 5-mm diameter steel bur with a stopper set designed for creating non-critical size defects under constant copious saline irrigation. Tibial intramedullary model rabbits were divided into 3 groups based on filling of defects with SPG-178 and β-TCP grafts, and no treatment (negative control) (n=15 for each material in 24 animals, Fig. 1A). The overlying soft tissues, periostium and fascia were sutured with catgut and the skin was treated with silk suture. Rabbits were euthanized 7 and 28 days after surgery for radiological and histological examinations and scanning electron microscopy (SEM) observation.

Lumbar posterolateral bone graft model

Rabbits were anesthetized with intramuscular administration of ketamine (0.7 ml/kg body weight) and xylazine (0.4 ml/kg body weight). Perioperative anesthesia was maintained by inhalation of isoflurane. Under sterile conditions, a longitudinal skin incision was performed, followed by exposure of the bilateral posterolateral lumbar spine (spinous process, lamina, and transverse process) at the L4/5 level. The bone chips and 0.8% SPG-178 hydrogel were mixed in a tube. Seven lumbar model rabbits were divided into 3 groups based on grafting with SPG-178 (200 µl) + bone chips (0.2 g) (n=5 defects), β-TCP (Sigma, 0.2 g) + bone chips (0.2 g) (n=5 defects), and bone chips only (0.2 g) (n=4 defects) on each side, after decortication with an airtome (Fig. 1B). Wounds were closed with size 5-0 nylon sutures. The same rabbit was used in an experimental group and the control group to eliminate the confounder of physiological variability among rabbits. Injections of enrofloxacin (5 mg/kg), an antibiotic, and meloxicam (0.6 mg/kg body weight), an anti-inflammatory analgesic, were administered intramuscularly for 3 days postoperatively. Animal monitoring was performed twice daily for 1 week after surgery, and then once daily until sacrifice after 56 days. A decrease in eating, drinking and moving or clear suffering from pain were defined as humane end points and animals would have been sacrificed immediately if these signs were exhibited. For sacrifice, animals were anesthetized with pentobarbital sodium (40 mg/kg) and perfused through the heart with 100 ml saline and

then 250 ml of 4% paraformaldehyde in phosphate buffer (pH 7.4).

Radiographic evaluation of bone repair

Tibia at 7, 14 and 28 days were imaged using digital X-ray (Softex, Tokyo, Japan) to evaluate new bone formation in defects before trimming and scanning with a Skyscan 176 micro-CT. At least three defects in each group were evaluated by X-ray at each time point. The volume of the defect area was quantified in mm^2. Samples were scanned at an energy of 55 kVp and intensity of 145 mA with 226 ms integration time, resulting in an isotropic voxel size of 36 mm. From the scanned volume, a cylindrical region of interest (ROI) corresponding to a defect size of 5-mm diameter at the site of the original defect was selected for analysis. After segmentation of the mineralized tissue with a threshold of 220, a Gauss filter width of 0.8, and filter support of 1.0, the mineralized matrix volume was quantified throughout the construct and is presented as bone volume in mm^3. β-TCP granules and remnants of free allogeneic bone were excluded from measurement of new bone. Micro-CT images were analyzed using the Image J color-threshold analyzer (National Institutes of Health, Bethesda, MD). White regions were assumed to indicate minimal tissue growth and grey regions to indicate maximal tissue growth. Quantitative analysis of new bone formation was carried out using the areas of these regions. In the spine model, the total fusion mass area was defined as the area around the L4/5 facet. New bone area was defined as the area with mineralized bone marrow within the mineralized area and osteoids attached to the hosted lamina. The evaluation was performed separately by two investigators in a blinded manner.

Histological analysis of bone repair in response to cell-seeded scaffolds

The most central and maximally sectioned surface of each tibial defect and the oblique view from the L4-5 transverse process to the lamina in the spine model was determined by hematoxylin and eosin staining of several of the serial 5-μm sections. Non-decalcified bones were embedded at low temperature in PMMA and serial 5-μm sections were stained with 5% silver nitrate (Von Kossa) and counterstained with 0.2% toluidine blue to distinguish mineral from soft tissue (Alizarin Red). Adjacent sections were stained with naphthol AS-TR phosphate (Sigma-Aldrich) in tris-maleate buffer pH 9.3 to identify alkaline phosphatase (ALP) activity in osteoblasts. The most central and maximally sectioned surface of each tibial defect and the oblique view from the L4-5 transverse process to the lamina in the spine model were subjected to histomorphometric analyses. Images of prepared slides were captured with a digital camera

(Olympus DP71, Tokyo) under a light microscope (Olympus BX60, Tokyo). Newly formed bone was marked, transformed into binary images, and quantified with Image J software, as previously described[1], before assessment based on trabecular bone forming the cortex close to the defect within the ROI. The area of newly formed bone was normalized using the area of the posterior cortex, where the surgical procedure had a minimal effect. This normalization helps to minimize the effects of differences in the size of tibia specimens among rabbits. The evaluation was performed separately by two investigators in a blinded manner.

Scanning electron microscopy

To evaluate grafted bone-host bone interactions, tibia intramedullary model constructs were processed for SEM evaluation (n=3). The bone constructs were fixed in 2% glutaraldehyde overnight at 4°C followed by phosphate-buffered saline overnight. Constructs were then postfixed in 2% osmium tetroxide for 2 h at 37°C, followed by dehydration using an ethanol series. Constructs were subjected to critical drying for 30 min before sticking onto metal stubs and gold coating in a sputter coater, followed by evaluation using SEM (JSM 7610F).

Statistical analysis

Statistical analysis was performed using SPSS (SPSS Inc., Chicago, IL, USA), using an unpaired two-tailed Student t test for single comparisons and one-way ANOVA with a post hoc Bonferroni test for multiple comparisons. In all analyses, significance was accepted at $p < 0.05$.

Results

Osteogenesis in the tibial intramedullary model

Radiological findings: Bone regeneration of scaffolds with different modifications and patterns was assessed *in vivo* after transplantation in the rabbit tibia model. Radiographs of implant sites at 7 (n=9), 14 (n=6), and 28 (n=4) days after surgery showed that both bone substitutes had incorporated surrounding bone (Fig. 2A). At 28 days, defects of the tibial condyle without bone substitute and with β-TCP were still empty, but those treated with SPG-178 were filled with new bone (Fig. 2B). Micro-CT analysis of transplants after 28 days (Fig. 3A) showed significantly greater newly formed bone matrix with SPG-178 (n=4) compared to β-TCP (n=4) and without treatment (n=4) (Fig. 3B).

Histology: Representative H&E and Alizarin red staining did not demonstrate clear new bone

formation in all groups at 7 days after implantation. Von Kossa staining showed marked new bone formation that was most prominent at the implanted SPG-178 (n=3) composite margin, compared with the β-TCP ($p<0.05$, n=3) and no treatment ($p<0.01$, n=3) groups. (Fig. 4A,B).

Bone morphology: SEM/3D micrographs using a steel bur immediately after surgery revealed the presence of erythrocytes in all groups (n=3) (Fig. 5A). Defects filled with SPG-178 showed erythrocytes penetrating into the hydrogel. At 7 days after surgery, collagen fibers and osteoblast proliferation were visible, especially in the cavity filled with SPG-178, which showed collagen fibers attached to host bone (Fig. 5B). After 28 days, SPG-178 samples showed significant restitution of the defect (Fig. 5C), whereas β-TCP samples had visibly less new bone formation.

Osteogenesis in the posterolateral lumbar bone graft model

Radiological findings: Bone regeneration of scaffolds with different modifications and patterns was assessed *in vivo* after transplantation in the rabbit spine model. Micro-CT of transplants after 56 days (Fig. 6AB) showed a tendency for a higher degree of newly formed bone matrix in the SPG-178 group compared to the β-TCP ($p=0.11$) and bone chips only ($p=0.18$) groups, but the difference was not significant (unpaired two-tailed Student t test).

Histology: Because the radiographic findings suggested that new bone formation in the spine model was increased by SPG-178 at 56 days after implantation, stimulated osteogenesis was examined microscopically by histological evaluation at this time point. Representative H&E, alkaline phosphatase (ALP), and Alizarin red staining showed clear new bone formation in the SPG-178 group (Fig. 7). Von Kossa staining showed that marked new bone formation attached to the lamina was most prominent at the implanted SPG-178 composite margin, compared with the β-TCP ($p<0.05$) and bone chips only ($p<0.01$) groups (Fig. 8).

Discussion

This *in vivo* study in rabbit spine and tibia models examined the progression and dynamics of bone healing using a self-assembling peptide hydrogel, SPG-178, as a scaffold, in comparison with β-TCP and bone chips in the spine model and no treatment in the tibia model. Radiographic analysis showed that SPG-178 induced a significant increase in new bone formation in both models, with attachment of new bone to host bone. Histological analyses of SPG-178 samples showed significantly more abundant newly formed bone, compared with the effect of β-TCP +

bone chips in the spine model and no treatment in the tibia model.

Several studies of RADA-16 hydrogels have suggested promotion of bone regeneration[16,19]. However, the self-assembling RADA16 peptide gel has a very low pH and may be cytotoxic to inner cells and host tissues. In contrast, SPG-178 hydrogel solution (2.4 mM) is transparent and forms a stable hydrogel at neutral pH when triggered by an increase in salt concentration. The stability of the peptide solution/hydrogel at neutral pH contributes to the biocompatibility of the scaffold. The solution can also be sterilized with an autoclave, which is advantageous in the sterilization procedure. SPG-178 hydrogel not only serves as a support for cells and growth factors, but has also been found to be highly conductive for the vascular system[11]. Several reports have described favorable effects of SPG-178 hydrogel in neurons and myoblasts in vitro[1,18] and Tsukamoto et al. found that dental pulp stem cells treated with the hydrogel had high potential for proliferation and differentiation into osteoblasts[26]. The present study provides the first evidence that SPG-178 hydrogel can act as a scaffold to increase new bone formation in rabbit spine and tibia models.

β-TCP is widely used in orthopedics as a bone substitute[3], due to calcium sulfate being released and absorbed quite rapidly *in vivo*. β-TCP scaffold materials are attractive as bone substitutes due to their biocompatibility, biological safety, essentially unlimited availability, ease of sterilization, and long shelf life[28]. B-TCP gives a good balance among absorption, degradation and new bone formation and can also preserve structural stability by releasing a large quantity of calcium (Ca^{2+}) and sulfate (SO_4^{2-}) ions, which are required inorganic salts for new bone formation[3,282,272,2626; 273,28]. In the present study, this degradation did not occur during formation of new bone, resulting in blocking of new bone formation (Figs. 2, 3, 4).

Factors necessary for bone formation include cells such as osteoblasts, an extracellular matrix to support adhesion and movement of these cells, and various intercellular functions such as storage of materials, a supply of nutrients (e.g., by angiogenesis) necessary for tissue formation, cytokines to promote and control cell growth, and dynamic factors such as strength and stability. Osteoblasts are activated by SPG-178 hydrogel and this hydrogel is suitable as a scaffold because charged amino acids in the peptide nanofiber, especially the positive arginine residues, support cell adhesion at the beginning of the culture[18,21]. Serum proteins in the cell culture medium may also attach to the peptide nanofiber and help with cell adhesion[23].

Interactions of positively charged amines in the polymer with the negative membrane improve

cell attachment and mobilization. A SEM image of a cavity filled with SPG-178 hydrogel showed erythrocytes penetrating into the hydrogel. At 7 days after surgery, collagen fibers and osteoblast proliferation were visible, and a micrograph of a cavity filled with SPG-178 hydrogel showed collagen fibers attached to host bone. After 28 days, samples treated with SPG-178 hydrogel showed significant restitution of the defect, whereas β-TCP had visibly less new bone formation. The radiographic and histology findings both showed that SPG-178 promoted attachment of the grafted bone to host bone. Therefore, use of SPG-178 seems to make it possible to maintain structure, even in bone defects, and to achieve good bone conduction. Vascular endothelial cells, bone marrow mesenchymal stem cells, and osteoblasts also appear to penetrate into the hydrogel from an early stage, allowing angiogenesis and osteogenesis to proceed[11].

There are several limitations in this study. First, the animals used were skeletally immature, and the bone may have had more osteoblastic potential than that of older animals. In addition, the sample number per model was limited. More extensive in vivo studies are required to prove that increased scaffold incorporation intrinsically promotes osteogenesis.

Conclusions

SPG-178 hydrogel is likely to be used in clinical applications because it has several benefits. These include favorable bone conduction properties, ability to act as a support for various cells and tissues, such as ECM, and ease of use to fill defects with complex shapes.

Acknowledgements

We thank K. Yamaguchi (Nagoya University) for her excellent technical assistance.

Funding

Financial support for this study was provided by the Japan Agency for Medical Research and Development (AMED) and JSPS KAKENHI Grant Number 15K10398 (to Kei Ando). The funders had no role in study design, data collection and analysis, decision to publish, or preparation of the manuscript.

Competing Interests

The authors have read the policy of the journal and wish to draw the attention of the editor to the following facts that may be considered as potential conflicts of interest and to significant financial contributions to this work. SPG-178 is a commercially available regent under the name of Panacea Gel^{TM} (Menicon Co., Ltd., Nagoya, Japan). Menicon Co., Ltd. offers its products at subsidized prices to Nagoya University. This does not alter the authors' adherence to all Bone policies on sharing data and materials.

1. Ando K, Imagama S, Ito Z, Kobayashi K, Hida T, Nakashima H, et al: Self-assembling Peptide Reduces Glial Scarring, Attenuates Posttraumatic Inflammation, and Promotes Neurite Outgrowth of Spinal Motor Neurons. **Spine (Phila Pa 1976) 41:**E1201-E1207, 2016
2. Ando K, Imagama S, Kobayashi K, Ito K, Tsushima M, Morozumi M, et al: Effects of a self-assembling peptide as a scaffold on bone formation in a defect. **PLoS One 13:**e0190833, 2018
3. Chang YL, Stanford CM, Keller JC: Calcium and phosphate supplementation promotes bone cell mineralization: implications for hydroxyapatite (HA)-enhanced bone formation. **J Biomed Mater Res 52:**270-278, 2000
4. Daculsi G, Laboux O, Malard O, Weiss P: Current state of the art of biphasic calcium phosphate bioceramics. **J Mater Sci Mater Med 14:**195-200, 2003
5. Davis ME, Motion JP, Narmoneva DA, Takahashi T, Hakuno D, Kamm RD, et al: Injectable self-assembling peptide nanofibers create intramyocardial microenvironments for endothelial cells. **Circulation 111:**442-450, 2005
6. Feuvrier D, Sagawa Y, Jr., Beliard S, Pauchot J, Decavel P: Long-term donor-site morbidity after vascularized free fibula flap harvesting: Clinical and gait analysis. **J Plast Reconstr Aesthet Surg 69:**262-269, 2016
7. Fischer CR, Cassilly R, Cantor W, Edusei E, Hammouri Q, Errico T: A systematic review of comparative studies on bone graft alternatives for common spine fusion procedures. **Eur Spine J 22:**1423-1435, 2013
8. Genove E, Shen C, Zhang S, Semino CE: The effect of functionalized self-assembling peptide scaffolds on human aortic endothelial cell function. **Biomaterials 26:**3341-3351, 2005
9. Hirano K, Matsuyama Y, Sakai Y, Katayama Y, Imagama S, Ito Z, et al: Surgical complications and management of occipitothoracic fusion for cervical destructive lesions in RA patients. **J Spinal Disord Tech 23:**121-126, 2010
10. Holmes TC, de Lacalle S, Su X, Liu G, Rich A, Zhang S: Extensive neurite outgrowth and active synapse formation on self-assembling peptide scaffolds. **Proc Natl Acad Sci U S A 97:**6728-6733, 2000
11. Hosseinkhani H, Hosseinkhani M, Khademhosseini A, Kobayashi H, Tabata Y: Enhanced angiogenesis through controlled release of basic fibroblast growth factor from peptide amphiphile for tissue regeneration. **Biomaterials 27:**5836-5844, 2006
12. Ishikawa K, Miyamoto Y, Nagayama M, Asaoka K: Blast coating method: new method of coating titanium surface with hydroxyapatite at room temperature. **J Biomed Mater Res 38:**129-134, 1997
13. Kang JS, Jeon YS, Ahn CH, Roh TH: Osteosynthesis versus endoprosthesis for the treatment of femoral neck fracture in Asian elderly patients. **BMC Musculoskelet Disord 17:**264, 2016
14. Kisiday J, Jin M, Kurz B, Hung H, Semino C, Zhang S, et al: Self-assembling peptide hydrogel fosters chondrocyte extracellular matrix production and cell division: implications for cartilage tissue repair. **Proc Natl Acad Sci U S A 99:**9996-10001, 2002

15. LeGeros RZ: Calcium phosphate-based osteoinductive materials. **Chem Rev 108:**4742-4753, 2008
16. Misawa H, Kobayashi N, Soto-Gutierrez A, Chen Y, Yoshida A, Rivas-Carrillo JD, et al: PuraMatrix facilitates bone regeneration in bone defects of calvaria in mice. **Cell Transplant 15:**903-910, 2006
17. Nagai Y, Unsworth LD, Koutsopoulos S, Zhang S: Slow release of molecules in self-assembling peptide nanofiber scaffold. **J Control Release 115:**18-25, 2006
18. Nagai Y, Yokoi H, Kaihara K, Naruse K: The mechanical stimulation of cells in 3D culture within a self-assembling peptide hydrogel. **Biomaterials 33:**1044-1051, 2012
19. Nakahara H, Misawa H, Yoshida A, Hayashi T, Tanaka M, Furumatsu T, et al: Bone repair using a hybrid scaffold of self-assembling peptide PuraMatrix and polyetheretherketone cage in rats. **Cell Transplant 19:**791-797, 2010
20. Parikh SN: Bone graft substitutes: past, present, future. **J Postgrad Med 48:**142-148, 2002
21. Schneider GB, English A, Abraham M, Zaharias R, Stanford C, Keller J: The effect of hydrogel charge density on cell attachment. **Biomaterials 25:**3023-3028, 2004
22. Semino CE, Merok JR, Crane GG, Panagiotakos G, Zhang S: Functional differentiation of hepatocyte-like spheroid structures from putative liver progenitor cells in three-dimensional peptide scaffolds. **Differentiation 71:**262-270, 2003
23. Seo JH, Matsuno R, Takai M, Ishihara K: Cell adhesion on phase-separated surface of block copolymer composed of poly(2-methacryloyloxyethyl phosphorylcholine) and poly(dimethylsiloxane). **Biomaterials 30:**5330-5340, 2009
24. Shang Q, Wang Z, Liu W, Shi Y, Cui L, Cao Y: Tissue-engineered bone repair of sheep cranial defects with autologous bone marrow stromal cells. **J Craniofac Surg 12:**586-593; discussion 594-585, 2001
25. Thaler M, Lechner R, Gstottner M, Kobel C, Bach C: The use of beta-tricalcium phosphate and bone marrow aspirate as a bone graft substitute in posterior lumbar interbody fusion. **Eur Spine J 22:**1173-1182, 2013
26. Tsukamoto J, Naruse K, Nagai Y, Kan S, Nakamura N, Hata M, et al: Efficacy of a Self-assembling Peptide Hydrogel, SPG-178-Gel, for Bone Regeneration and Three-dimensional Osteogenic Induction of Dental Pulp Stem Cells. **Tissue Eng Part A**, 2017
27. Walsh WR, Vizesi F, Michael D, Auld J, Langdown A, Oliver R, et al: Beta-TCP bone graft substitutes in a bilateral rabbit tibial defect model. **Biomaterials 29:**266-271, 2008
28. Wang J, Chen W, Li Y, Fan S, Weng J, Zhang X: Biological evaluation of biphasic calcium phosphate ceramic vertebral laminae. **Biomaterials 19:**1387-1392, 1998
29. Yokoi H, Kinoshita T, Zhang S: Dynamic reassembly of peptide RADA16 nanofiber scaffold. **Proc Natl Acad Sci U S A 102:**8414-8419, 2005
30. Zhang S, Gelain F, Zhao X: Designer self-assembling peptide nanofiber scaffolds for 3D tissue cell cultures. **Semin Cancer Biol 15:**413-420, 2005
31. Zhang S, Holmes T, Lockshin C, Rich A: Spontaneous assembly of a self-complementary oligopeptide to form a stable macroscopic membrane. **Proc Natl Acad Sci U S A 90:**3334-3338, 1993

32. Zhang S, Holmes TC, DiPersio CM, Hynes RO, Su X, Rich A: Self-complementary oligopeptide matrices support mammalian cell attachment. **Biomaterials 16:**1385-1393, 1995

Figure Legends

Fig. 1. (A) Tibial intramedullary model. (B) Lumbar spine model.

Fig. 2. Radiographic evaluation of the tibia intramedullary model. Defects of the tibial condyle treated without bone substitute and with β-TCP remained empty at 28 days, but those treated with SPG-178 were filled new bone ($p<0.05$ vs. no treatment, $p=0.01$ vs. β-TCP) (7 days n=9, 14 days n=6, 28 days n=4).

Fig. 3. Micro-CT analysis of transplants in the tibia model. (A) Micro-CT analysis of transplants in the tibia model after 7days showed the same size. (A, B) The defects after 28 days showed significantly more new bone matrix in the SPG-178 (n=3) group compared to the β-TCP (n=3) and no treatment (n=3) groups although.

Fig. 4. Histological evaluation of the tibia intramedullary model. (A) H&E and Alizarin red staining showed clear new bone formation in the SPG-178 group in the tibia model. (B) Von Kossa staining showed that the SPG-178 group (n=3) had a higher amount of calcium compared to the β-TCP(n=3) and no treatment(n=3) groups.

Fig. 5. SEM/3D micrographs of the tibia intramedullary model. (A) SEM/3D micrographs of osteotomies prepared using a steel bur immediately after surgery revealed the presence of erythrocytes in all groups. The micrograph of the cavity filled with SPG-178 showed erythrocytes penetrating into hydrogel (arrow). (B) At 7 days, collagen fibers and osteoblast proliferation were visible, especially in the cavity filled with SPG-178, which had collagen fibers attached to host bone (arrow). (C) At 28 days, SPG-178 samples showed significant restitution of the defect (arrow), whereas β-TCP samples had less new bone formation.

Fig. 6. Micro-CT of the rabbit spine model. (A, B) Micro-CT indicated a tendency for more new bone matrix (arrow head) in the SPG-178 group compared to the β-TCP ($p=0.11$) and bone chips

only (p=0.18) groups in the spine model.

Fig. 7. Histological findings at 56 days after implantation in the rabbit spine model. New bone formation around the defect was increased in SPG-178 samples. H&E, alkaline phosphatase, and Alizarin red staining showed new bone formation in the SPG-178 group (arrows).

Fig. 8. Von Kossa staining in the rabbit spine model. (A, B) Von Kossa staining showed a higher amount of calcium in the SPG-178 group compared to the β-TCP and bone chips only groups in the rabbit spine model.